A&A 615, A161 (2018)
https://doi.org/10.1051/0004-6361/201832885

Astronomy & Astrophysics

Lucky Spectroscopy, an equivalent technique to Lucky Imaging

Spatially resolved spectroscopy of massive close visual binaries using the *William Herschel* Telescope

J. Maíz Apellániz[1], R. H. Barbá[2], S. Simón-Díaz[3,4], A. Sota[5], E. Trigueros Páez[1,6], J. A. Caballero[1], and E. J. Alfaro[5]

[1] Centro de Astrobiología, CSIC-INTA, Campus ESAC, Camino bajo del castillo s/n, 28692 Vill. de la Cañada, Madrid, Spain
e-mail: jmaiz@cab.inta-csic.es
[2] Departamento de Física y Astronomía, Universidad de La Serena, Av. Cisternas, 1200 Norte La Serena, Chile
[3] Instituto de Astrofísica de Canarias, 38 200 La Laguna, Tenerife, Spain
[4] Departamento de Astrofísica, Universidad de La Laguna, 38 205 La Laguna, Tenerife Spain
[5] Instituto de Astrofísica de Andalucía-CSIC, Glorieta de la Astronomía s/n, 18008 Granada, Spain
[6] Departamento de Física, Ingeniería de Sistemas y Teoría de la Señal, Escuela Politécnica Superior, Universidad de Alicante, Carretera San Vicente del Raspeig s/n, 03690 San Vicente del Raspeig, Alicante, Spain

Received 23 February 2018 / Accepted 6 April 2018

ABSTRACT

Context. Many massive stars have nearby companions whose presence hamper their characterization through spectroscopy.
Aims. We want to obtain spatially resolved spectroscopy of close massive visual binaries to derive their spectral types.
Methods. We obtained a large number of short long-slit spectroscopic exposures of five close binaries under good seeing conditions. We selected those with the best characteristics, extracted the spectra using multiple-profile fitting, and combined the results to derive spatially separated spectra.
Results. We demonstrate the usefulness of Lucky Spectroscopy by presenting the spatially resolved spectra of the components of each system, in two cases with separations of only ∼0.″3. Those are δ Ori Aa+Ab (resolved in the optical for the first time) and σ Ori AaAb+B (first time ever resolved). We also spatially resolve 15 Mon AaAb+B, ζ Ori AaAb+B (both previously resolved with GOSSS, the Galactic O-Star Spectroscopic Survey), and η Ori AaAb+B, a system with two spectroscopic B+B binaries and a fifth visual component. The systems have in common that they are composed of an inner pair of slow rotators orbited by one or more fast rotators, a characteristic that could have consequences for the theories of massive star formation.

Key words. binaries: spectroscopic – binaries: visual – methods: data analysis – stars: early-type – stars: massive – techniques: spectroscopic

1. Introduction

The Galactic O-Star Spectroscopic Survey (GOSSS, Maíz Apellániz et al. 2011) is obtaining R ∼2500, signal-to-noise ratio $S/N \gtrsim 200$, blue-violet spectroscopy of all optically accessible O stars in the Galaxy. To date, three survey papers (Sota et al. 2011, 2014; Maíz Apellániz et al. 2016, from now on GOSSS I+II+III) have been published with a total of 590 O stars[1]. O stars love company and few (if any) of them is born completely isolated. As a result, their multiplicity fraction, both visual and spectroscopic is close to one (see GOSSS II). This characteristic can be a blessing, allowing for the measurement of masses through their orbits, but most times is also a curse, as multiplicity can be hard to identify and resolve (spatially or spectroscopically) and its hidden nature introduces biases when calculating properties such as the initial mass function (Maíz Apellániz 2008) and produces spectral peculiarities that may be mistaken for unique characteristics of the target.

Lucky Imaging (Law et al. 2006; Baldwin et al. 2008; Smith et al. 2009) is a high-spatial resolution passive imaging technique that takes a large number of short exposures and selects those with the best quality. It combines these best-quality exposures to produce a final result with a full width at half maximum (FWHM) much better than the seeing that would be obtained in a long exposure. In a strict sense, Lucky Imaging requires that one reaches the diffraction limit and that places restrictions on the wavelength used (z and i bands are preferred over shorter wavelengths), the telescope size (small telescopes yield larger diffraction-limited point spread functions (PSFs) but large telescopes have a lower probability of producing good images, so a 2–4 m telescope is the best choice), and integration time (which must be at least similar to the atmospheric coherence time determined by turbulence). In a looser sense, we can still call Lucky Imaging a setup in which some of those requirements are not met, yielding a final product with a FWHM improved over that of a long exposure but not reaching the diffraction limit. It is that sense that will be used here.

[1] The GOSSS spectra are being gathered with six facilities: the 1.5 m Telescope at the Observatorio de Sierra Nevada (OSN); the 2.5 m du Pont Telescope at Las Campanas Observatory (LCO); the 3.5 m Telescope at the Observatorio de Calar Alto (CAHA); and the 2.0 m Liverpool Telescope (LT), the 4.2 m *William Herschel* Telescope (WHT), and the 10.4 m Gran Telescopio Canarias (GTC) at the Observatorio del Roque de los Muchachos (ORM). Of those, the LT is a recent addition to the mix.

Table 1. Multiple systems observed in this paper.

System	Comp.	n_{exp}	n_{used}	t_{exp}	Sep.	PA	Δm
ζ Ori	AaAb+B	100	12	0.1 s	2.″42	167°	2.3
σ Ori	AaAb+B	100	7	1.0 s	0.″26	70°	1.2
15 Mon	AaAb+B	110	17	1.0 s	3.″00	214°	3.1
δ Ori	Aa+Ab	100	10/6	0.1 s	0.″30	131°	1.3
η Ori	AaAb+B	100	29/22	1.0 s	1.″80	77°	1.3

Notes. For each system we give the total number of exposures, the number of exposures used (with two values when the system was observed on two nights), and the single exposure time. The systems separation, position angle, and approximate magnitude difference were obtained from the Washington Double Star Catalog (Mason et al. 2001) and our own AstraLux data (Maíz Apellániz 2010)

Lucky Spectroscopy is the logical extension of Lucky Imaging to spectroscopy: obtaining a large number of short long-slit spectroscopic exposures under good-seeing conditions, selecting those with the best characteristics, and combining them to derive spatially resolved spectra of two or more closely separated point sources aligned with the slit. In this paper we describe how we have done precisely that for five massive visual multiple systems observed with the WHT as part of GOSSS.

2. Data and methods

We obtained spectra for five multiple massive-star systems (Table 1) on the night of 2017 September 7 and repeated the observations on the following night for two of them (δ Ori Aa+Ab and η Ori AaAb+B). The spectra were obtained with the standard GOSSS configuration for the Intermediate dispersion Spectrograph and Imaging System (ISIS) at the WHT (see Table 1 in GOSSS III) with three modifications:

- A slit width of 0.″5 was used instead of the standard 0.″9 to increase the spectral resolution to $R \sim 4000$.
- A narrow window of 116 pixels (33.″2 at 0.″20/pixel) in the spatial direction was used to read the CCD in just 15 s.
- Either 100 or 110 short exposures of 0.1 s or 1 s each were obtained for each target.

Each of the 100–110 exposures of a given object was extracted individually by fitting a two-component one-dimensional Moffat profile to model the PSF, that is, by spatially deconvolving the spectrum at each wavelength. The separation between the two components was kept fixed from the known astrometry (Table 1) and common values of α and β (the Moffat profile parameters) were used for both components. The characteristics of the PSF were allowed to change as a function of wavelength but an average profile was generated by subsampling the pixel scale by a factor of 10 using the drizzle method (Fruchter & Hook 2002), recentering, and collapsing the result in wavelength. As the trace crosses multiple times from one pixel to another and we have almost 4000 valid wavelength points, each subsampled pixel receives ~400 contributions and the spectral information is erased in the collapsed result. From the collapsed profile we measured the mean magnitude difference Δm, the mean seeing (defined as the FWHM of the profile for a single component), and a χ^2 value for the fit that measures its goodness.

Typically for Lucky Imaging, a measurement of the seeing in each frame is obtained and a given fraction (e.g. 1% or 10%) of the best frames are selected to produce the final combined image. Here we follow a similar strategy but using the three parameters above (Δm, seeing, and χ^2) as conditions instead of just the seeing. Given that our sample of stars is small and that the number of frames is not too large, we selected the criteria to be applied to each system by (a) looking at the individual exposures one by one and (b) then selecting a reasonable criterion for each system. Examples of this two-step procedure are shown in Fig. 1. One important difference in the case of Lucky Imaging is that we combined our selected spectra after extracting and normalizating them as opposed to selecting the best frames first and then combining them prior to extraction. We were able to do so because of our previous knowledge about the expected separation and Δm and the high S/N present in the individual exposures compared to a typical Lucky Imaging situation.

After obtaining the spectrograms, we performed the spectral classification with MGB (Maíz Apellániz et al. 2012, 2015) and a new grid of spectroscopic standards that includes B-type stars (Maíz Apellániz et al., in prep.). The spectrograms in Figs. 2 and 3 and spectral types in Table 2 are available from the Galactic O-Star Catalog (GOSC, Maíz Apellániz et al. 2004, 2017)[2].

3. Results

We present our results here. We also compare them to the previously available information for each system.

ζ Ori AaAb+B = Alnitak AaAb+B = 50 Ori AaAb+B = HD 37 742 AB+HD 37 743 = BD −02 1338 AaAb+B = ALS 14 793 AB+ALS 16 893. ζ Ori is Orion's Belt easternmost star and a a multiple system with three close bright visual components (Aa, Ab, and B) and a fourth distant (53″) dim one (C) that will not be considered here. Ab is a very close optical companion in a seven-year orbit that is always less than 50 mas away from Aa and is fainter by 2 mag (Hummel et al. 2013), so the pair cannot be spatially resolved in our data and only a combined AaAb spectral type can be derived. The B component is 2.″424 away (Maíz Apellániz 2010) and is 2.3 mag fainter than the combined light of AaAb[3]. In our data we resolve B from AaAb, something that we already did using conventional techniques in GOSSS I+II. The spectral type we derive for AaAb is identical to that of GOSSS II, O9.2 IbNwk var. That of B is slightly different: the spectral subtype changes from O9.5 to O9.7, the luminosity class from II-III to III, and the rotation index from (n) to n. The new n rotation index for the B component is consistent with the value of $v \sin i$ of 350 km s^{-1} measured by Hummel et al. (2013). The B spectrogram has a very good S/N and no sign of residual contamination from AaAb. In this case, Lucky Spectroscopy improves previous results using conventional techniques by reducing the contamination of the primary on the secondary.

σ Ori AaAb+B = 48 Ori AaAb+B = HD 37 468 AaAb+B = BD −02 1326 AaAb+B = ALS 8473 AaAb+B. The σ Ori system is a sexdecuple system surrounded by its homonymous open cluster (Caballero 2014). The three brightest stars, Aa, Ab, and B are all contained within 0.″3, with the rest of the components located at significantly larger separations. The B component is in a nearly circular orbit around AaAb with a period of 159.90 a and a current separation of 0.″26 (Schaefer et al. 2016). The Aa and Ab components form a binary whose existence was

[2] GOSC has been recently moved to http://gosc.cab.inta-csic.es but the old URL (http://gosc.iaa.es) will be temporarily kept as a mirror.

[3] Due to an undiscovered typo, the Δm was given as exactly 2.424 in GOSSS I+II. The actual magnitude difference cannot be expressed with such precision unless a specific wavelength is specified.

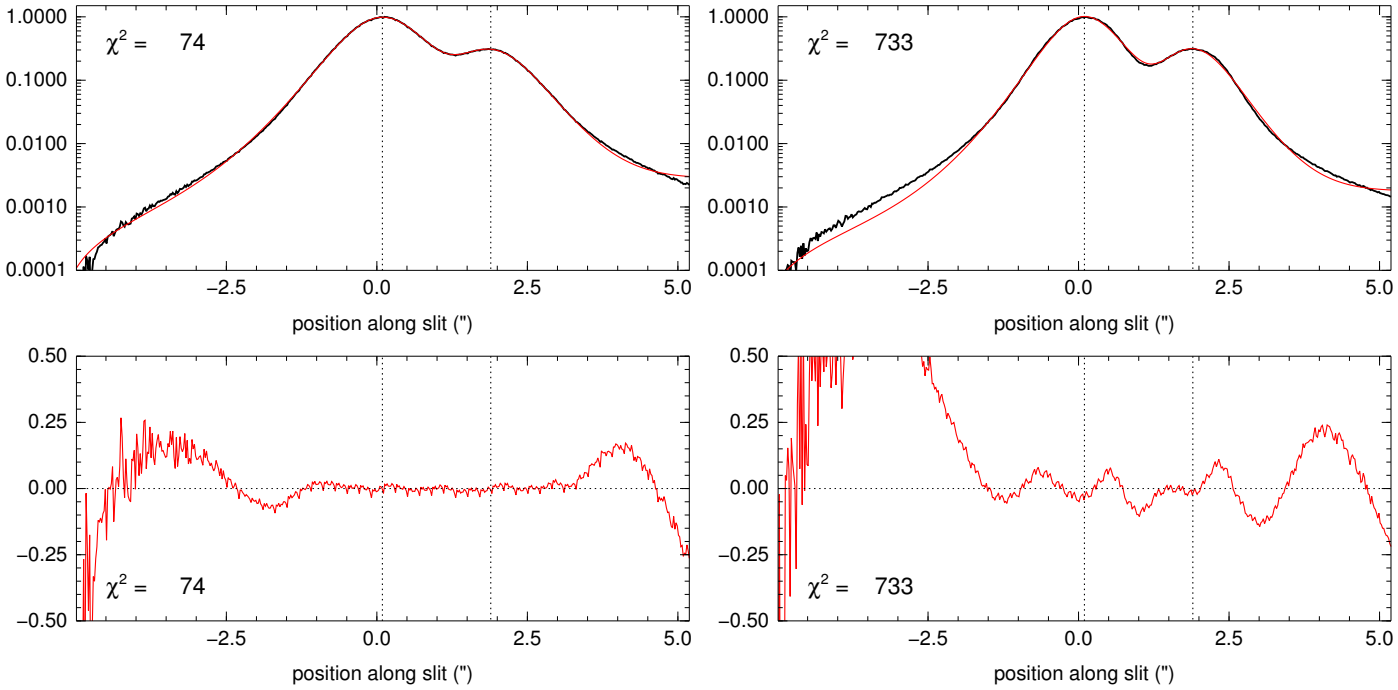

Fig. 1. *Top panel*: comparison between subsampled collapsed spatial profiles for a selected exposure (*left panel*) and a rejected one (*right panel*) for the 2017 September 7 observations of η Ori AaAb+B. Solid black is used for the observed profile, solid red for the fit, and dotted black for the star positions. *Bottom panel*: same as top panels but for the normalized residual i.e. (observed-fit)/fit. The selected exposure has a more symmetric profile than the rejected one, yielding a much lower χ^2 and a reduced contamination of the primary on the secondary.

Table 2. New spectral classifications.

Name	GOSSS ID	RA (J2000)	Dec (J2000)	ST	LC	Qual.	Second.
ζ Ori AaAb	GOS 206.45−16.59_01	05:40:45.527	−01:56:33.26	O9.2	Ib	Nwk var	...
ζ Ori B	GOS 206.45−16.59_02	05:40:45.571	−01:56:35.59	O9.7	III	n	...
σ Ori AaAb	GOS 206.82−17.34_01	05:38:44.765	−02:36:00.25	O9.7	V	...	...
σ Ori B	GBS 206.82−17.34_02	05:38:44.782	−02:36:00.27	B0.2	V	(n)	...
15 Mon AaAb	GOS 202.94+02.20_01	06:40:58.656	+09:53:44.71	O7	V	((f))z var	...
15 Mon B	GBS 202.94+02.20_02	06:40:58.546	+09:53:42.23	B2:	V	n	...
δ Ori Aa	GOS 203.86−17.74_01	05:32:00.398	−00:17:56.69	O9.5	II	Nwk	...
δ Ori Ab	GOS 203.86−17.74_02	05:32:00.414	−00:17:56.91	O9.7	III:	(n)	...
η Ori AaAb	GBS 204.87−20.39_01	05:24:28.617	−02:23:49.69	B0.7	V	...	B1.5: V
η Ori B	GBS 204.87−20.39_02	05:24:28.729	−02:23:49.32	B1	V	(n)	B1 V(n)

Notes. GOS/GBS stands for Galactic O/B Star. The information in this table is also available in electronic form at the GOSC web site (http://gosc.cab.inta-csic.es).

not confirmed through spectroscopic means until very recently (Simón-Díaz et al. 2011). The Aa+Ab system has an eccentric orbit with a period of 143.198 d (Simón-Díaz et al. 2015a) that has been resolved with interferometry (Schaefer et al. 2016). We have been able to spatially resolve B from AaAb, which to our knowledge had never been done with spectrosccopy before, making it the system in this paper resolved with the smallest separation. The σ Ori AaAb spectrum in Fig. 2 has a very good S/N and yields a combined spectral type of O9.7 V. The spectral subtype is the same as the one in GOSSS II, but the luminosity class there is III instead of V. As discussed in GOSSS III, we expected that previous luminosity classification to be the result of the contamination from B, given the young age of the system, and our results here confirm that (see also Simón-Díaz et al. 2015b, where they catch the spectroscopic binary with a large velocity difference and are able to provide separate information for Aa and Ab; it is our intention to reobserve the system with Lucky Spectroscopy at such a moment to provide separate spectral types for Aa and Ab). The σ Ori B spectrum is noisier, as expected for the dimmer companion of a spatially deconvolved system, but there are no strong signs of contamination from AaAb (e.g. compare Si III λ4552 for the two of them). We have derived a spectral type of B0.2 V(n), which is consistent with the expected result from Simón-Díaz et al. (2015b), in terms of both spectral type and rotational velocity.

15 Mon AaAb+B = S Mon AaAb+B = HD 47 839 AaAb+B = BD +10 1220 AaAb+B = ALS 9090 AaAb+B. 15 Mon is similar to σ Ori in that it is a system with many components inside a small cluster, NGC 2264 (Walker 1956; Rebull et al. 2002) The three brightest stars, Aa, Ab, and B are all contained within 3″,

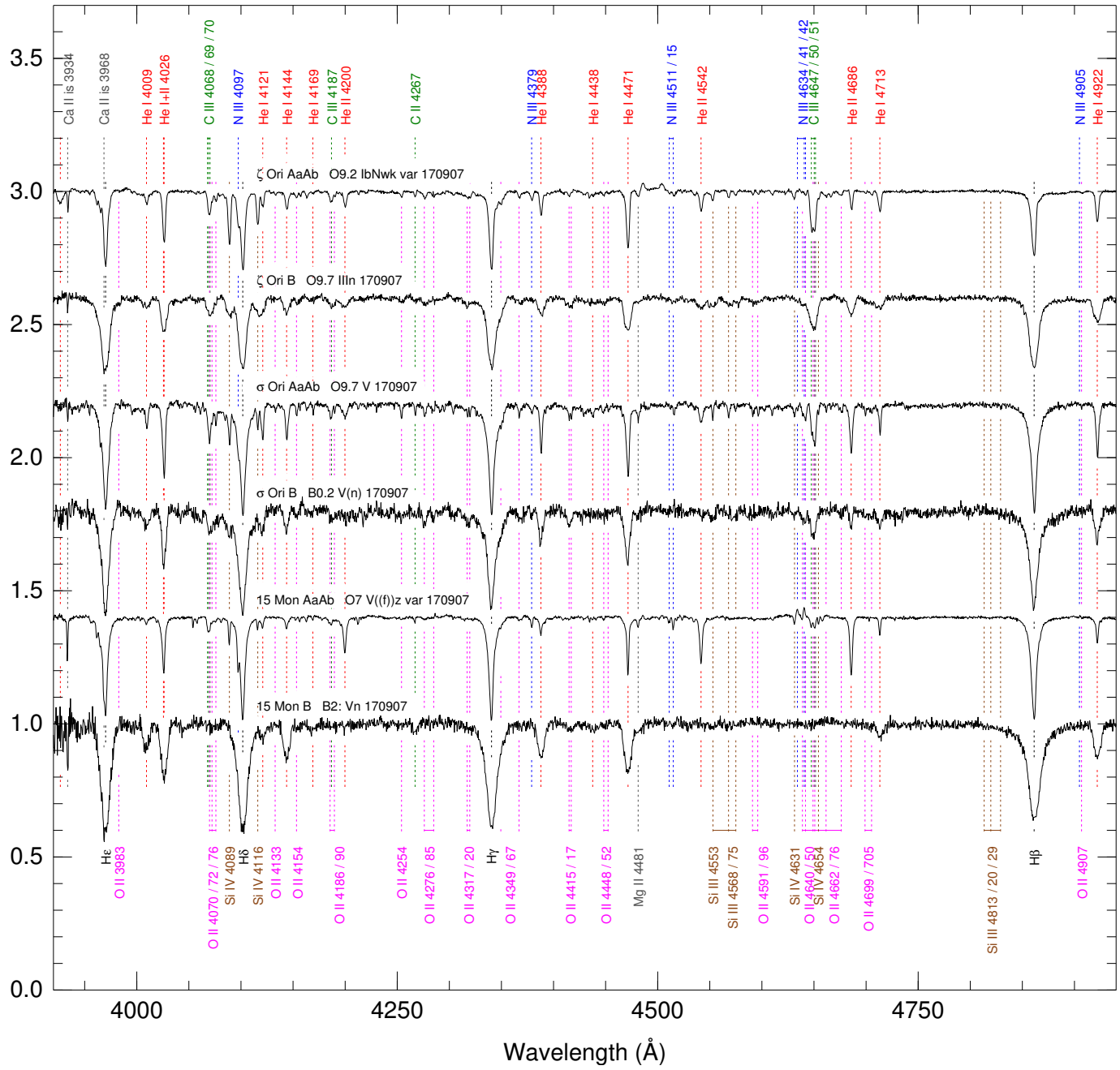

Fig. 2. Spectrograms for the three systems observed on a single epoch at the original spectral resolution ($R \sim 4000$) and on the stellar reference frame. For each spectrogram, the name, spectral type, and evening date (YYMMDD) are shown. Main atomic lines are indicated.

with the rest of the components located at significantly larger separations. The inner pair Aa+Ab has a Δm of 1.2 mag, is currently separated by 0.″1, and its orbit is rather uncertain, with a high eccentricity and a period measured in decades (Gies et al. 1997; Cvetković et al. 2010). The B component is located 3″ away from AaAb and the Δm is 3.1 magnitudes, the largest difference in our sample. Our data cannot resolve Aa and Ab but we obtain separate spectra for AaAb and B, something that we did previously using conventional techniques in GOSSS I+II. The AaAb spectrogram has an excellent S/N and its spectral type is the same as our previous GOSSS one, O7 V((f))z var. The variability may be due to the profile differences caused by the orbit of Ab around Aa. For the B component, we had previously obtained different spectral classifications as a late O or an early B star due to the limitations of the conventional techniques. With Lucky Spectroscopy we establish it is an early B star with a classification of B2: Vn, which is consistent with the observed Δm. The uncertainty in the spectral subtype is due to the relatively poor S/N of the deconvolved spectrum. There are no signs of contamination from AaAb. as the two spectra have very different rotational velocities: B is a fast rotator while the combined AaAb spectrum shows very narrow lines.

δ Ori Aa+Ab = Mintaka Aa+Ab = 34 Ori Aa+Ab = HD 36 486 A+B = BD −00 983 A+B = ALS 14 779 A+B. δ Ori is Orion's Belt westernmost star and a multiple system at the center of the Mintaka cluster (Caballero & Solano 2008). It has two close bright visual components (Aa and Ab) and two distant dim ones (B and C) that will not be considered here. Aa is

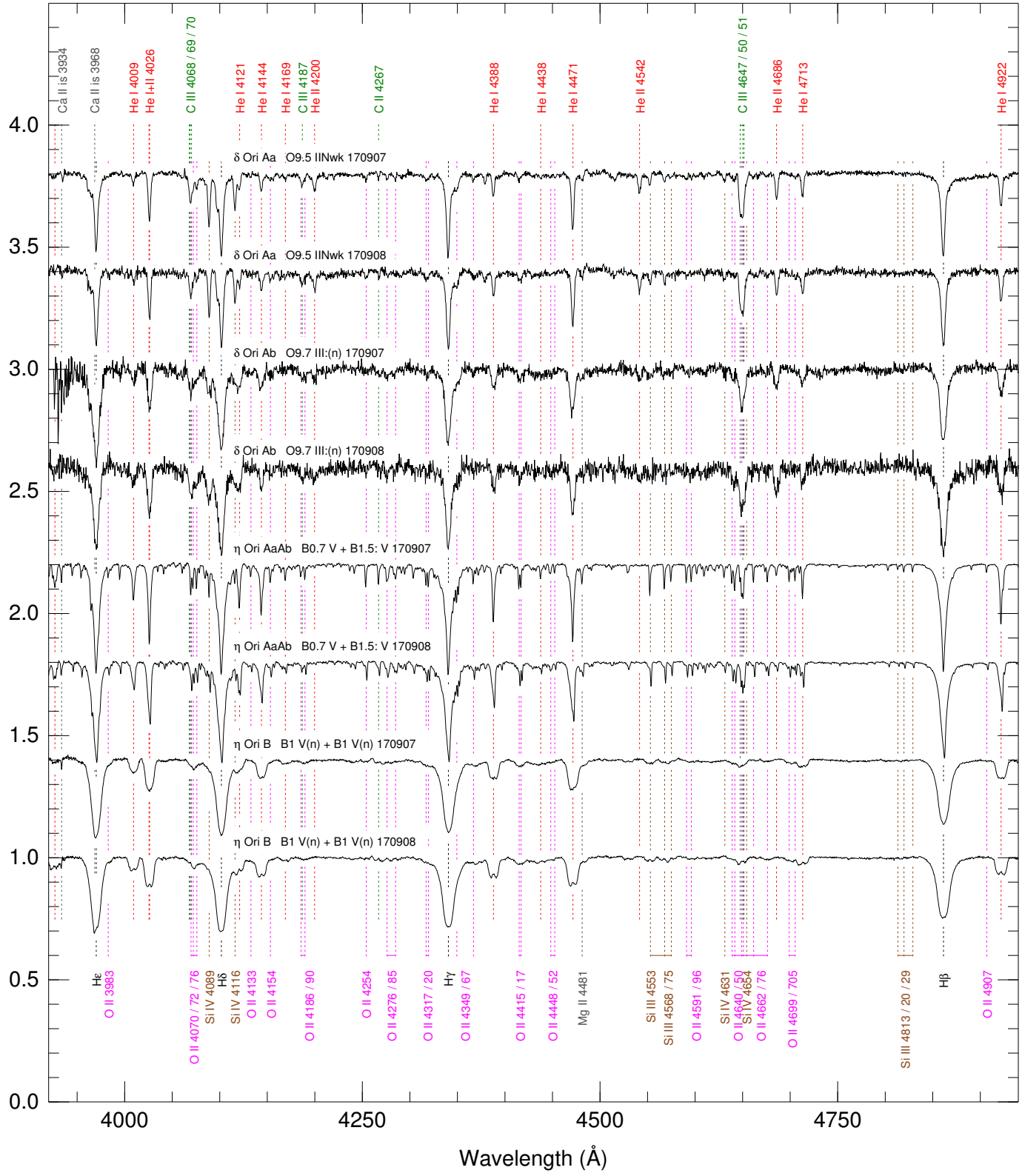

Fig. 3. Same as Fig. 2 for the two systems observed on 2017 September 7 and 8.

itself composed of two spectroscopic components (Aa1+Aa2) in an eclipsing orbit with a 5.7325 d period, while Ab is two magnitudes fainter than the two Aa components and located 0.″267 away in 1993 and moving away from the primary (Hartmann 1904; Harvin et al. 2002). We observed the system on two consecutive nights and in both cases we were able to spatially resolve Ab from Aa, this being one of the two systems in this paper (σ Ori is the other one) where the power of Lucky Spectroscopy becomes more apparent. The two spectra for Aa yield the same spectral type as for the combined Aa+Ab value from GOSSS I, O9.5 IINwk, but the lines are slightly narrower. When analyzing the data for GOSSS I, the combined spectrum was close to

being (n), something that does not happen for the spatially resolved spectra (this has the additional advantage of giving us a more pure spectrum for a classical O9.5 II classification standard). There are very small variations between the two epochs for Aa, likely due to the motion of Aa1 and Aa2 but the signature of the latter in the combined spectrum is very weak (Shenar et al. 2015). The two epochs for Ab yield the same spectral type, O9.7 III:(n), and in both cases there are indications of only a slight residual contamination from Aa, with the second epoch being noisier. The (n) qualifier indicates that Ab is a fast rotator, as previously noted by Harvin et al. (2002) and Shenar et al. (2015). The differences between the spectral types of Aa (Aa1+Aa2) and Ab are consistent with the $T_{\rm eff}$ and $\log g$ differences measured by Shenar et al. (2015) using spectral disentangling (as opposed to the spatial deconvolution used here). Richardson et al. (2015) also spatially resolved Aa and Ab in the UV using HST/STIS and obtained very similar values of $T_{\rm eff}$ around 31 kK for Aa1 and Ab, with error bars close to 2000 K, which is also consistent with our spectral classifications. That paper using UV data is the only one we have found where δ Ori Aa+Ab was spatially deconvolved, making our result the first time it has been done in the optical.

η Ori AaAb+B = 28 Ori AaAb+B = HD 35 411 AaAb+B = BD −02 1235 AaAb+B = ALS 14 775 AaAb+B. η Ori is a multiple system with no associated open cluster (Caballero & Solano 2008) and with three close bright visual components (Aa, Ab and B) and a distant dim one (C) that will not be considered here. The Aa+Ab pair has a separation of less than 0.″1 and a Δm of 1.5 mag in a 9.442 a orbit (Balega et al. 1999), making it too close to be resolved in our data. On the other hand, B is separated from the AaAb system by 1.″8 with a Δm of 1.3 mag, making it a relatively easy target for Lucky Spectroscopy (Δm similar to σ Ori AaAb+B or δ Ori Aa+Ab but at a larger separation). η Ori AaAb+B differs from the other four systems in this paper in not including an O star (it had not appeared in a GOSSS paper before) and in having a complex photometric curve. One photometric period is 7.989255 d long and is associated with the eclipsing binary Aa (unresolved components Aa1+Aa2, Waelkens & Lampens 1988; De Mey et al. 1996) while a second, shorter one, has an unclear origin. It has been proposed that it originates in B being another eclipsing binary with a 0.864 d period (Waelkens & Lampens 1988; Lee et al. 1993), but it has not been proved conclusively, as other alternatives are possible and no spectrum of B separated from AaAb had been previously published. In our Aa+Ab spectrograms two narrow-lined B-type components are seen, with the weak component moving redwards with respect to the strong one in the 1.023 d elapsed between the two epochs. The derived spectral types are B0.7 V and B1.5: V, and both move in opposite directions between the two epochs, indicating that they correspond to the two components in Aa, the 7.989255 d spectroscopic binary. The Ab component leaves no apparent signal in the spectrum, even though it could easily do it with a Δm of 1.5 mag. One possibility is that it is a fast rotator (see Simón-Díaz et al. 2015a for the discussion of this possibility for σ Ori B, which we have confirmed here). The B spectrograms show two nearly identical spectroscopic components; two fast rotators with spectral types B1 V(n). The two epochs are relatively similar but the velocity spacing between the two components is larger in the second one (440 ± 20 km s^{-1}) than in the first one (380 ± 20 km s^{-1}). If the period is 0.864 d, the epoch difference would correspond to 1.18 periods i.e. the stars would have completed a little over one orbit, with the first epoch corresponding to a point just before quadrature and the second epoch to a point just after quadrature. With such a short period and large velocity differencess the two stars must be in a contact or overcontact configuration with a large inclination, making eclipses unavoidable and thus confirming the origin of the Lee et al. (1993) light curve. More epochs are needed to study this system in depth. It could become a future gravitational wave source if both components explode as SNe independently or a stellar merger if the fusion takes place before that point. In summary, η Ori is a complex quintuple system of which four (the two spectroscopic components in Aa and the two in B) have confirmed early-B spectral types and the fifth (Ab) is also likely to fall in the same category.

4. Summary and future work

We have used Lucky Spectroscopy to obtain spatially resolved spectra of five close massive multiple systems, two of them for the first time (one in the optical and the other in any range), and in the process established the validity of the technique. In four cases (ζ Ori, σ Ori, 15 Mon, and δ Ori) we have the same configuration: a hierarchical triple system with an inner pair composed of two slow rotators and an outer component that rotates significantly faster than the other two. For the fifth system (η Ori), there is also an inner pair made up of two slow rotators but with an intermediate orbit (that of Ab) where the large rotational velocity is only suspected and an outer system that is itself a pair of fast rotators. This pattern may be related to the formation mechanisms of massive stars, indicating that the less massive outer object tends to either be the result of mergers or in some other way absorb additional rotational angular momentum. Finally, if we combine the results of GOSSS I+II+III with the recent ones of Maíz Apellániz et al. (2018), we are left with the following statistics for the project: 594 O-type systems, 24 of early type other than O (B, A supergiants, sdO, PNN), and eleven of later types. Having demonstrated the validity of Lucky Spectroscopy, we plan to use it again with a larger sample to test its limits. As with most techniques that extract information from two closely separated point sources, there is likely a region in the separation-Δm plane where the technique works well and another one where it does not. The results here indicate that Lucky Spectroscopy with our setup is capable of separating stars 0.″3 apart if Δm is small and stars 3″ apart with a $\Delta m \approx 3$ but more observations are needed to map the feasibility boundary. Another line of work we plan to explore is the use of an electron-multiplying CCD as a detector to reach fainter objects.

Acknowledgements. As we were about to submit this paper, we received the sad news of the death of Nolan R. Walborn after a long battle with cancer. As he was the inspiration for GOSSS, we would like to dedicate this paper to him. May he rest in peace. This work has made use of the Washington Double Star Catalog (Mason et al. 2001). The authors would like to thank the personnel of the Isaac Newton Group of telescopes for their support throughout the years, with a special mention to Cecilia Fariña for her help with the setup for Lucky Spectroscopy. The first author is amazed that the instrument he used for his PhD Thesis is still working one quarter of a century later and is not yet surpassed in some of its characteristics. We acknowledge support from the Spanish Government Ministerio de Economía y Competitividad (MINECO) through grants AYA2016-75 931-C2-1/2-P (J.M.A., A.S., E.T.P., and E.J.A), AYA2015-68 012-C2-1/2-P (S.S.-D. and E.T.P.) and AYA2016-79 425-C3-2-P (J.A.C.). R.H.B. acknowledges support from the ESAC Faculty Council Visitor Program.

References

Baldwin, J. E., Warner, P. J., & Mackay, C. D. 2008, A&A, 480, 589
Balega, I. I., Balega, Y. Y., Hofmann, K.-H., Tokovinin, A. A., & Weigelt, G. P. 1999, Astron. Lett., 25, 797
Caballero, J. A. 2014, Observatory, 134, 273
Caballero, J. A., & Solano, E. 2008, A&A, 485, 931

Cvetković, Z., Vince, I., & Ninković, S. 2010, New Ast., 15, 302
De Mey, K., Aerts, C., Waelkens, C., & Van Winckel H. 1996, A&A, 310, 164
Fruchter, A. S., & Hook, R. N. 2002, PASP, 114, 144
Gies, D. R., Mason, B. D., Bagnuolo, Jr., W. G., et al. 1997, ApJ, 475, L49
Hartmann, J. 1904, ApJ, 19
Harvin, J. A., Gies, D. R., Bagnuolo, Jr. W. G., Penny, L. R., & Thaller, M. L. 2002, ApJ, 565, 1216
Hummel, C. A., Rivinius, T., Nieva, M.-F., et al. 2013, A&A, 554, A52
Law, N. M., Mackay, C. D., & Baldwin, J. E. 2006, A&A, 446, 739
Lee, W. B., Sung, E. C., Koch, R. H., et al. 1993, ASP Conf. Ser., 38, 239
Maíz Apellániz, J. 2008, ApJ, 677, 1278
Maíz Apellániz, J. 2010, A&A, 518, A1
Maíz Apellániz, J., Pérez, E., & Mas-Hesse, J. M. 2004, AJ, 128, 1196
Maíz Apellániz, J., Sota, A., Walborn, N. R., et al. 2011, HSA, 6, 472
Maíz Apellániz, J., Pellerin, A., Barbá, R. H., et al. 2012, ASP Conf. Ser., 465, 484
Maíz Apellániz, J., Alfaro, E. J., Arias, J. I., et al. 2015, HSA, 8, 603
Maíz Apellániz, J., Sota, A., Arias, J. I., et al. 2016, ApJS, 224, 4
Maíz Apellániz, J., Alonso Moragón, A., Ortiz de Zárate Alcarazo, L., & The GOSSS Team. 2017, HSA, 9, 509
Maíz Apellániz, J., Pantaleoni González, M., & Barbá, R. H. 2018, A&A, in press, DOI: 10.1051/0004-6361/201832787
Mason, B. D., Wycoff, G. L., Hartkopf, W. I., Douglass, G. G., & Worley, C. E. 2001, AJ, 122, 3466
Rebull, L. M., Makidon, R. B., Strom, S. E., et al. 2002, AJ, 123, 1528
Richardson, N. D., Moffat, A. F. J., Gull, T. R., et al. 2015, ApJ, 808, 88
Schaefer, G. H., Hummel, C. A., Gies, D. R., et al. 2016, AJ, 152, 213
Shenar, T., Oskinova, L., Hamann, W.-R., et al. 2015, ApJ, 809, 135
Simón-Díaz, S., Caballero, J. A., & Lorenzo, J. 2011, ApJ, 742, 55
Simón-Díaz, S., Caballero, J. A., Lorenzo, J., et al. 2015a, ApJ, 799, 169
Simón-Díaz, S., Negueruela, I., Maíz Apellániz, J., et al. 2015b, HSA, 8, 581
Smith, A., Bailey, J., Hough, J. H., & Lee, S. 2009, MNRAS, 398, 2069
Sota, A., Maíz Apellániz, J., Walborn, N. R., et al. 2011, ApJS, 193, 24
Sota, A., Maíz Apellániz, J., Morrell, N. I., et al. 2014, ApJS, 211, 10
Waelkens, C., & Lampens, P. 1988, A&A, 194, 143
Walker, M. F. 1956, ApJ, 124, 668